Numerical modeling of performance of olive seeds as permeable reactive barrier for containment of copper from contaminated groundwater

Ziad T. Abd Ali[a,*], Hussain M. Flayeh[b], Mohammed A. Ibrahim[c]

[a]*Department of Environmental Engineering, College of Engineering, University of Baghdad, Baghdad, Iraq, Tel. +9647903433954, email: z.teach2000@yahoo.com (Z.T.A. Ali)*
[b]*Department of Environmental Engineering, College of Engineering, University of Baghdad, Baghdad, Iraq, email: Hussmf200211@yahoo.com (H.M. Flayeh)*
[c]*Department of Civil Engineering, College of Engineering, University of Al-Nahrain, Baghdad, Iraq, email: moh_env@yahoo.com (M.A. Ibrahim)*

ABSTRACT

This study investigates the performance of olive seeds as a reactive medium in the permeable reactive barrier (PRB) for removing of copper from a simulated contaminated groundwater. The effect of different parameters such as contact time, initial pH of the solution, agitation speed, initial copper concentration, and sorbent dosage was studied in batch experiments. The best values of these parameters that achieved the maximum removal percent (99%) of copper were 70 min, 5.5, 250 rpm, 10 mg/l, and 0.8 g/50 ml, respectively. The leaching test indicated that the dissolution of copper-bearing olive seeds is very low. A two-dimensional groundwater numerical model was developed under equilibrium condition to evaluate the performance of two configurations of PRBs namely continuous (C-PRB) and funnel and gate (FG-PRB). The results of batch experiments, leaching test, and 2D numerical model proved that the olive seeds barrier was efficient in the restriction of contaminant plume and both configurations of PRBs can be used successfully to treat copper-contaminated groundwater with operation time equal to 170 and 100 d for C-PRB and FG-PRB, respectively.

Keywords: Olive seeds; Copper; Permeable reactive barrier; Groundwater

1. Introduction

The contamination of groundwater by organic and inorganic compounds has been considered since the industrial revolution. Groundwater(water found beneath the surface of the ground and seeped down from the surface by migrating through the soil matrix and spaces in geologic formations) is generally more reliable for use than surface water [1]. Heavy metals including copper do not undergo biological decomposition and can accumulate in living organisms then interfering with the natural functioning of ecosystems [2]. The most common technology used for remediation of groundwater has been ex-situ pump-and-treat system. This system extract groundwater to the surface then treats it through different approaches such as adsorption and either re-introduce the treated water to the subsurface or discharge it to a storm drain. This technique is difficult, costly, and ineffective most of the time in removing enough contamination to restore the groundwater to drinking water standards in acceptable time frames. Accordingly, permeable reactive barriers (PRBs) technology was the alternative method used to remediate groundwater contaminated with different types of contaminants. It is found to be more cost-effective than a pump and treat and has been a demonstrated potential to diminish the spread of contaminants [3]. PRB technology may be installed as a continuous reactive barrier (C-PRB) or as a funnel-and-gate system (FG-PRB). Due to the fact that one of the most important stages of designing a PRB is choosing appropriate filler for the barrier, many research centers are searching for new reactive materials

*Corresponding author.

in order to improve the effectiveness of decontamination [4]. Activated carbon can be used as a reactive medium (sorbent) in PRB because of its effectiveness in removal of a wide variety of organic and inorganic pollutants from different media, but it still very expensive. Therefore, the production of low-cost sorbents becomes the aim of many researchers [5]. So, there are many effective alternative materials have been used as reactive materials in PRB in many research, some have used waste as low-cost materials [6–8], and others have made effective carbon from low-cost materials [9,10]. However, this research did not explain the extent of the difference in the performance of the PRB as C-PRB andFG-PRB, which is one of the worthy aspects of this study. In addition,the development of low-cost adsorbent from olive seeds as an inexpensive and efficient reactive material to use it in two configurations of PRB for removing of copper from polluted groundwater. The performance evaluation of the proposed PRBs was achieved using a numerical groundwater model.

2. Materials and methods

2.1. Mediums and contaminant

Olive seeds were chosen as a reactive medium for PRB. It was first dried and sieved to the particle sizes of 1–0.6 mm for the preparation of activated carbon by chemical activation using phosphoric acid. Approximately 100 g of olive seeds were impregnated with 400 ml of phosphoric acid solution with a concentration of 0 wt.%. The mixture stirred at 85°C maintaining for 6 h to ensure a completed reaction between phosphoric acid and olive seeds. After mixing, the mixture was then filtered and the remaining solids were dried at 105°C for about 24 h. The acid-impregnated olive seeds were placed in a furnace at a temperature of 500°C for 2 h under the nitrogen flow of 200 mL/min. Then they were cooled down to the room temperature and washed sequentially several times with hot distilled water until the pH of the washing solution reached a value between 6 and 7. Finally, they were dried at 110°C for 24 h and weighed to calculate the activated carbon yield [11]. The properties of this medium have been measured at the Petroleum Research and Development Center such as BET surface area = 11×10^5 m^2/kg, bulk density = 910 kg/m^3, porosity = 0.53, and hydraulic conductivity = 7.4×10^{-5} m/s.

The properties of Iraqi sandy soil were used as an aquifer in a numerical groundwater model to simulate copper transport in groundwater because it represents the worst case in the speed of the arrival of the pollutant into the groundwater. This soil had a particle size distribution ranged from 63 μm to 0.71 mm (porosity = 0.41) with an effective grain size, d_{10}, of 110 μm, a median grain size, d_{50}, of 180 μm, a uniformity coefficient, $C_u = d_{60}/d_{10}$, of 1.73, and hydraulic conductivity of 4.2×10^{-5} m/s.

The salt of $Cu(N0_3)_2$ (manufactured by BDH, England) was used in the preparation of the copper stock solution by dissolving it at a known concentration in distilled water. The solutions used for this study were obtained by dilution of the stock solution to the required concentration. The initial pH of each of the solutions was adjusted by the addition of HNO_3 or NaOH solution. The initial concentrations of

the copper and the corresponding concentrations after fixed time periods were measured by an atomic absorption spectrophotometer (AAS) (Shimadzu, Japan).

2.2. Scanning electron microscopy analysis

The scanning electron microscopy (SEM) is one of the most widely used instruments in materials research laboratories. Scanning electron microscopy is central to micro structural analysis and therefore important to any investigation relating to the processing, properties, and behavior of materials that involves their microstructure. Therefore, the olive seeds were examined using SEM (Inspect S50 Model, FEI/ Netherlands).

2.3. Fourier-transform infrared analysis

The Fourier transfer infrared spectroscopy (FTIR) analysis has been considered as a kind of direct mean for identifying the characteristic functional groups on the surface of the olive seeds, which are responsible for contaminant binding [12]. The characteristic bands of the olive seeds before and after copper uptake at a pH of 5.5 were used to assess the changes in the functional groups. A 200 ml flask filled with 50 ml of the copper solution with a concentration of 10 mg/l and 0.8 g of olive seeds was agitated for an equilibrium time at 250 rpm, and then the infrared spectra of the olive seeds samples before and after copper sorption were examined using Shimadzu FTIR, 8000 series spectrophotometer, Japan.

2.4. Distilled water leaching of copper-bearing olive seeds

To confirm the ability of the olive seeds to maintain the copper that removed from the contaminated solution. Copper-bearing olive seeds specimens were subjected to a distilled water leaching procedure, conducted in accordance with "German Standard Methods DIN 38414 Part 4" [13]. The leachates were analyzed for the copper.

2.5. Batch experiments

The batch tests are carried out to specify the best conditions of contact time, initial pH of the solution, initial copper concentration, dosage of olive seeds, and agitation speed. Series of 200 ml flasks are employed. Each flask is filled with 50 ml of a copper solution which has an initial concentration of 50 mg/L. About 0.7 g/50 ml of olive seeds was added to different flasks and these flasks were kept stirred in the high-speed orbital shaker at 100 rpm for 120 min. A fixed volume (20 ml) of the solution was withdrawn from each flask. This withdrawn solution was filtered to separate the olive seeds and a fixed volume (10 ml) of the clear solution was pipetted out to determine the concentration of the remaining copper in the solution. Kinetic studies were investigated with different values of pH (3.5, 4.5, 5.5, and 6.6), different values of initial concentration of copper (50, 40, 30, 20 and 10 mg/L), amounts of olive seeds dosage (0.2, 0.4, 0.6, 0.7, 0.8, and 1 g/50 ml) and finally values of agitation speed (100, 150, 200 and 250 rpm).

From the best experimental results, the amount of copper retained on the solid phase (olive seeds), q_e, was calculated using Eq. (1) [14]:

$$q_e = (C_o - C_e)\frac{V}{m} \qquad (1)$$

where C_o and C_e are the initial and equilibrium concentrations of copper in the solution (mg/L), V is the volume of solution in the flask (L), and m is the mass of sorbent material (olive seeds) in the flask (g).

2.6. Description of sorption data

For the description of sorption data, two isotherm models were used. A summary of these models was presented by "Hamdaoui and Naffrechoux" [15] as follows:

The Langmuir model can be expressed as in Eq. (2):

$$q_e = \frac{q_m b C_e}{1 + b C_e} \qquad (2)$$

where q_m is the maximum sorption capacity (mg/g), b (L/mg) is the constant related to the free energy of sorption, C_e (mg/l) is the equilibrium concentration of copper in the bulk solution, and q_e (mg/g) is the amount of contaminant sorbed per unit weight of sorbent at equilibrium.

The Freundlich model is given by Eq. (3):

$$q_e = K_F C_e^{\frac{1}{n}} \qquad (3)$$

where n is an empirical coefficient indicative of the intensity of the sorption and K_F is the Freundlich sorption coefficient.

2.7. Longitudinal dispersion coefficient

The effect of hydrodynamic dispersion is to cause a plume of contamination to elongate in the direction of advection as well as to develop a gradient of decreasing concentration from the center to the margins of the plume.

However, the values of longitudinal dispersivity (α_L) used in the present study for PRB (olive seeds) and aquifers (sandy soil) were estimated using the following equation [16]:

$$\alpha_L = 0.83 (\log \log L)^{2.414} \qquad (4)$$

where L is the length of the flow path (m).

Tortuosity is a measure of the effect of the shape of the flow path followed by water molecules in a porous medium. It is calculated depending on the porosity of the medium (n) as follows [17]:

$$\tau = n^{m-1} \qquad (5)$$

Archie (1942) reports values for m [Eq. (5)] of 1.8–2 for consolidated sandstones, 1.3 for unconsolidated sand in a laboratory experiment, and 1.3–2 for partly consolidated sand. For theoretical or conceptual work the value $m = 2$ is considered, which may be justified if there is no further information as cited by Holzbecher [17].

2.8. Two-dimensional model development

The numerical modeling of simulated copper transport in groundwater was performed in a sandy unconfined aquifer model. A two-dimensional groundwater model for this aquifer was set up using COMSOL Multiphysics 3.5a software which is based on finite element method. The model aquifer is contained within the square shape (50 m × 50 m), it consists of two types of the PRB of interest in this study namely continuous PRB (C-PRB) and funnel and gate PRB (FG-PRB) as shown in Fig. 1. The C-PRB model aquifer consisted of three parts. The first part represented by 30 m length of the sandy soil measured from the left side of the aquifer, the second part represented by 3 m (thickness) barrier of olive seeds placed beside the soil, and 17 m of the sandy soil represented the third part was placed beside the barrier. The contaminant
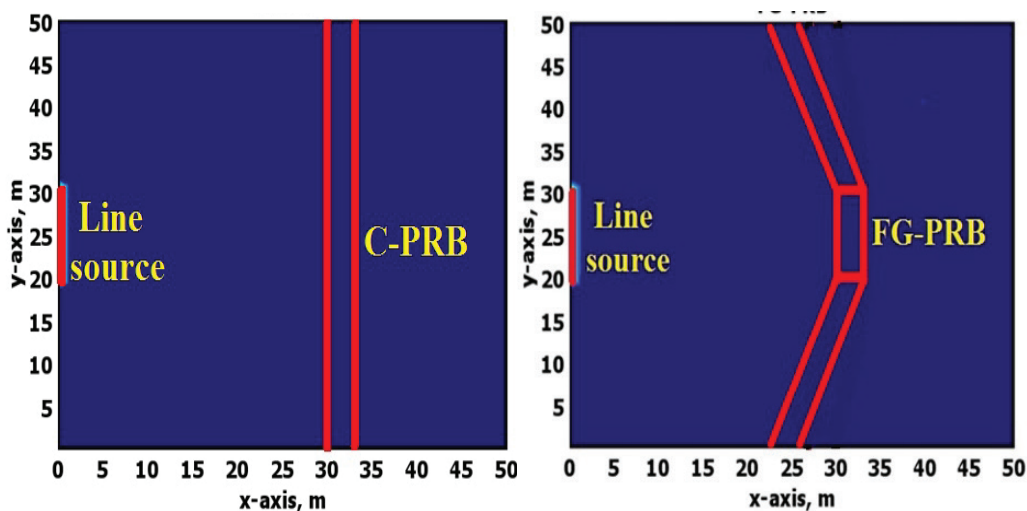

Fig. 1. Schematic diagram of the model aquifer with PRBs.

solution with an initial concentration and velocity of 0.01 kg/m³ and 3.45 m/d was introduced through the model aquifer from line source (10 m long) which was located at left side of the aquifer. This source was simulated a continuous release of contamination, therefore, at zero time, the concentration of the pollutant in all aquifer model, except the line source, is zero then the concentrations of pollutant start to increase with the increase of time indicating the spread of the pollutant in the aquifer model. The concentrations of copper at points of interest were monitored in front of, within, and behind the PRB, these points are very important because they clarify the difference in pollutant concentrations before, during, and after treatment (i.e. before, during, and after PRB) thus demonstrating the efficiency of the barrier. In the C-PRB, the reactive media was placed along the barrier (i.e., 50 m long) with thickness of 3 m, while for FG-PRB, shorter reactive media was installed only in the permeable gate part of the barrier (i.e., 10 m long) with the same thickness of 3 m, and the impervious material such as ebonite (impermeable material) was installed in the impermeable funnel parts, therefore groundwater flow and contaminant transport were intentionally allowed through the gate part only.

2.9. Transport of contaminant through the model aquifer

The contaminant migration in a porous medium is due to the advection-dispersion processes; therefore, considering a two-dimensional system (unidirectional fluid flow and two-dimensional transient solute transport), the dissolved copper mass balance equation can be written as follows:

$$D_x \frac{\partial^2 C}{\partial x^2} + D_y \frac{\partial^2 C}{\partial y^2} - V_x \frac{\partial C}{\partial x} = R \frac{\partial C}{\partial t} \qquad (6)$$

where C represents copper concentration in water, D_x and D_y are the hydrodynamic dispersion coefficient in the x and y directions (m²/s), respectively, V_x is the seepage velocity in the x-direction (m/s), x and y are the distance in the x and y-direction (m), respectively, t is the time (s), and R is known as the retardation factor, it represents the effect of retarding the transport of sorbed species relative to the advection front.

As a result of sorption processes, some solutes (pollutants) will move much more slowly through the aquifer than the groundwater that is transporting them, this effect is called retardation, it is expressed mathematically in advection-dispersion equation [Eq. (6)] by retardation factor (R) [16]. For the flow of contaminated groundwater through the sandy soil (aquifer), the value of R will be assumed equal to 1 which is reasonable for this medium (assumed as non-reactive medium). On the other hand, the sorption of copper on olive seeds (PRB) is governed by a Langmuir isotherm model, as illustrated in section (3.5), so that the retardation factor is expressed as:

$$R = 1 + \frac{\rho_b}{n} \left(\frac{q_m b}{(1+bC)^2} \right) \qquad (7)$$

where ρ_b, n are the bulk density and porosity of the barrier, respectively.

To present a numerical solution, Eq. (6) in combination with initial and boundary conditions (Table 1) can be solved using COMSOL Multiphysics 3.5a.

3. Results and discussion

3.1. Scanning electron microscopy (SEM) analysis

The external surface of the olive seeds before and after carbonization process using SEM Scanning electron microscopy is given in Fig. 2. The surface of the olive seeds before carbonization (Fig. 2a) was quite smooth without any porous structure except for some occasional cracks or curves. While the morphology of olive seeds after carbonization (Fig. 2b) was different, this image shows an irregular and heterogeneous surface morphology, it is obvious that the olive seeds after carbonization have cavities and cracks on their external surfaces. It seems that the cavities on the surfaces of olive seeds resulted from the evaporation of the activating agent (phosphoric acid) during carbonization process, leaving the space previously occupied by the activating agent [11].

3.2. Fourier-transform infrared analysis

The FTIR spectrums of olive seeds samples after and before copper sorption were examined. The displacement in the infrared frequencies supports that alcohols, carboxylic acid, amine, ester, aromatic and alkyl- halides are the functional groups causing the sorption of copper onto olive seeds as shown in Fig. 3, Table 2 [8]. Accordingly, the mechanisms that controlled the sorption of copper by using olive seeds may be the adsorption process supported by the presence of the functional groups described previously.

3.3. Distilled water leaching of copper-bearing olive seeds

According to the "German Standard Methods", the leaching test indicated that the dissolution of copper-bearing olive seeds is generally very low (below the limits of detection). This result confirms that olive seeds can be effective reactive material in PRB by bonding strongly with the contaminant and prevent it to turn into a liquid phase again.

Table 1
Boundary and initial conditions used in the model aquifer (Fig. 1)

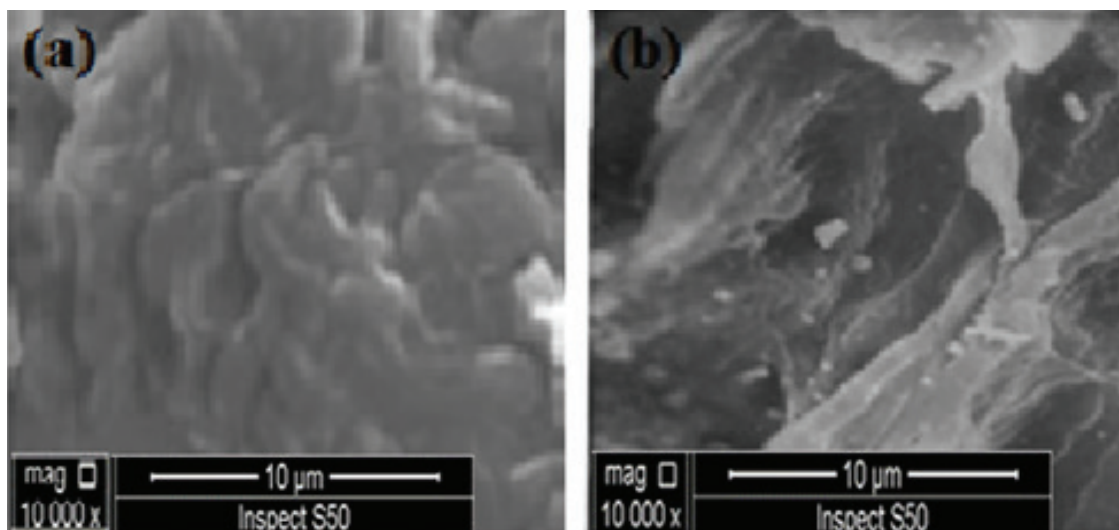| Item	Location		Type/ Value
Boundary conditions	Upper boundary		No flux/symmetry
	Lower boundary		No flux/symmetry
	Left side boundary	Except for the line source	No flux/symmetry
		Line source	$C_o = 0.01$ kg/m³
	Right side boundary		Advective flux = 0
Initial condition	(X,Y)		$C_o = 0$

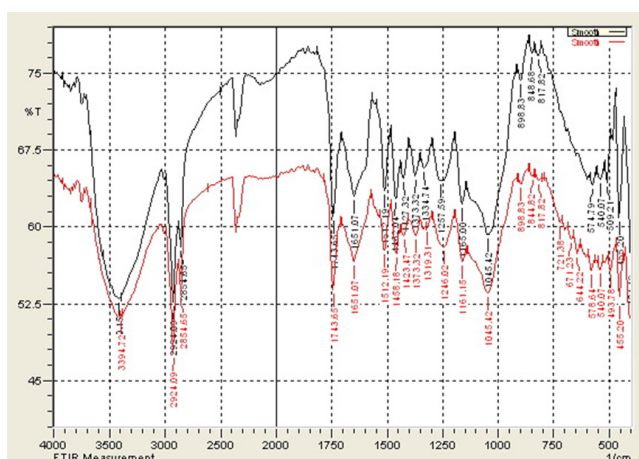Fig. 2. SEM images of olive seeds (mag. 10 000×) (a) before carbonization (b) after carbonization.

Fig. 3. FTIR spectrum of olive seeds before and after loading with copper.
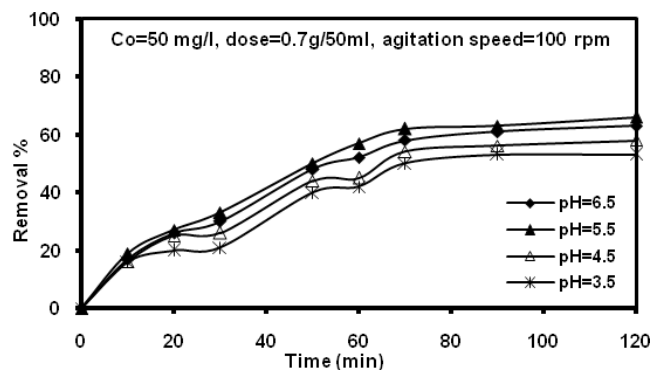

Fig. 4. Removal percent of copper on olive seeds as a function of contact time and initial pH.

3.4. Influence of batch operating parameters

3.4.1. Effect of contact time and initial pH of the solution

The effect of the initial pH of the solution and the contact time on copper sorption is illustrated in Fig. 4 where 0.7 g of olive seeds was added to 50 ml of copper solution at 25°C. As the Fig. 4 shows, in the beginning, the increasing rate of adsorption was fast as the contact time increased till reaching the equilibrium time (70 min), this could be as a result of the availability of many adsorbent sites for the copper adsorption. After that, the adsorption rate was reduced because of the decreasing of the remaining vacant surfaces. It is clear that at pH of 5.5 the removal percent of copper was at its maximum value. An increase or decrease in the pH from this value resulted in a reduction of the removal percent. This may be due to competition for binding sites between copper ions and protons at low pH values, while at higher pH, the solubility of complexes decreases sufficiently allowing precipitation which may complicate the adsorption process and does not bind to the sorption sites on the surface of the olive seeds [18].

Table 2
Functional groups responsible for copper sorption onto olive seeds

Functional group	Type of bond	Wave No. (cm^{-1}) before Cu(II) loading	Wave No. (cm^{-1}) after Cu(II) loading
Alcohols	N–H$_2$ stretch	3410.15	3394.72
Carboxylic acids	O–H bend	1462.04	1458.18
Amines	C–N stretch	1334.74	1319.31
Esters	C–C(O)–C stretch	1257.59	1246.02
Aromatic	C–H bend	848.68	844.82
Alkyl halides	–C–Br stretch	574.79	578.64

3.4.2. Effect of agitation speed

The agitation speed test is not crucial for the application in the PRB, but it is an important element in the batch experiments to find the best speed achieve the highest removal to reduce the time of experiments, otherwise, the experiments can take longer time. As illustrated in Fig. 5, with the increase of the rate of shaking, the uptake of copper increases. On increasing agitation speed from 100 to 250 rpm, there is a gradual increase in copper uptake at which about (77%) of the copper is removed. This can be due to improving the diffusion of copper towards the surface of the reactive medium (olive seeds) and more contact between the binding sites and the copper in the solution.

3.4.3. Effect of Initial copper concentration

Fig. 6 presents the effect of initial concentration of copper on its removal percent. It shows that when decreasing the initial concentration of copper from 50 to 10 mg/L, the removal percent increased from 77 to 88.2 %, this represents the saturation of the active sites available on the olive seeds to interact with copper, so with decreasing concentration the more favorable sites became involved in the process [19].

3.4.4. Effect of olive seeds dosage

The effect of olive seeds dosage on the removal percent of the copper was examined at different dosages. These dosages were ranging from 0.2 to 1 g and added to 50 mL of the

copper solution as presented in Fig. 7. This figure showed that the increase of the olive seeds dosage from 0.2 to 0.8 g at fixed initial copper concentration will lead to improving the removal percent because of a higher dosage of olive seeds in the solution leads to greater availability of sorption sites. It's also clear that after a dosage of 0.8 g, the removal percent was not changed. Hence, even with the further addition of olive seeds, the removal percent of copper remain constant (99%).

3.5. Sorption isotherms

The parameters which gave the higher removal percent of copper (99%) were pH of 5.5, agitation speed of 250 rpm, an equilibrium time of 70 min, an initial concentration of 10 mg/L, and olive seeds dosage of 0.8 g/50 mL. The results of the sorption experiment were fitted with the previously described linearized form of two isotherm models. The fitted parameters and coefficient of determination (R^2) for each model are illustrated in Table 3. In comparison with the two models, the Langmuir isotherm model provided the higher coefficient of determination, therefore the Langmuir isotherm model was used to describe the copper sorption in the partial differential equation (PDE) governing the transport of a copper in two-dimension (2D) continuous model which is solved using COMSOL Multiphysics 3.5a. Considering the sandy soil (aquifer) as a non- reactive medium (inert) is one of the main aspects of the present study. Therefore the batch experiments included the copper with olive seeds only without sandy soil.
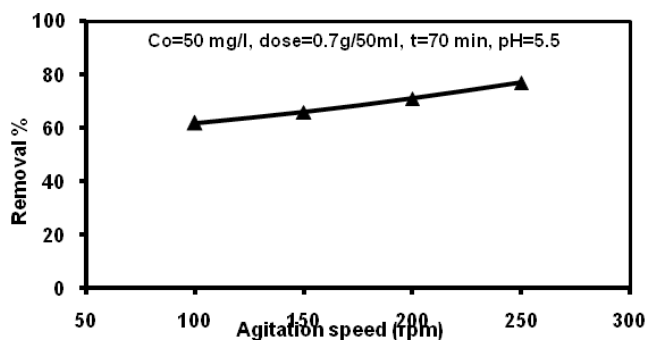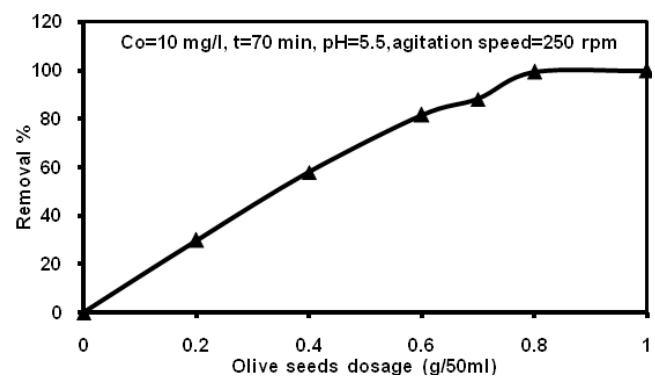

Fig. 5. Effect of agitation speed on removal percent of copper.
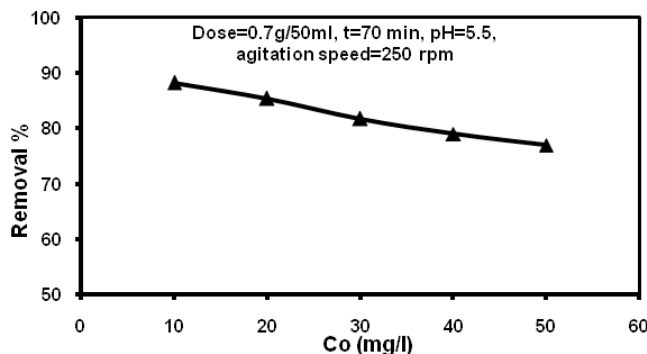
Fig. 6. Effect of initial copper concentration on removal percent of copper onto olive seeds.

Fig. 7. Effect of olive seeds dosage on removal percent of copper.

Table 3
Parameters of isotherm models for sorption of copper onto olive seeds

Isotherm models	Parameter	
Langmuir	b (L/mg)	0.1360
	q_m (mg/g)	3.9961
	R^2	0.9971
Freundlich	K_F (mg/g)(L/mg)$^{1/n}$	3.7110
	n	9.320
	R^2	0.9733

3.6. Transport of copper through the model aquifer

Fig. 8 describes the predicted contour plot of transport of copper-contaminated groundwater with $C_0 = 0.01$ kg/m³ and velocity = 3.45 m/d across the model aquifer in three cases (without PRB, with C-PRB, and with FG-PRB) after 1, 3, 160, and 500 d. It is clear that the direction of the transport process of copper is from high concentration gradient on the left-hand side to the lower ones on the right-hand side, and the copper-contaminated groundwater is transported from the contaminated site to the PRBs within 160 d without exceeding the barrier in comparison with the first case (without PRB), which mean that the propagation of contaminated plume is restricted by the olive seeds in the barrier region.

3.7. Performance of PRBs

After reaching the PRB of olive seeds, the copper-contaminated groundwater is treated such that its concentration is reduced by the sorption process. For two configurations of PRBs (C-PRB andFG-PRB), the typical results for this simulation were obtained in term of the relationship between copper concentration and PRB operation time. The relationship between time and concentration of copper entering (inflow) and leaving (outflow) the PRB is shown in Fig. 9. As expected, for two configurations of PRBs, there are clearly evident that the concentrations of copper entering the PRBs were constant at about 0.0078 kg/m³ which are less than the concentrations at the source (i.e., 0.01 kg/m³). This is probably because of the effect of dispersion. The main results that can be drawn from this figure that both configurations of PRBs can be used successfully to treat copper-contaminated groundwater, and

the PRBs starts to saturate with increasing the travel time and this means that the copper retardation factor was reduced, indicating a decrease in the percentage of barrier (olive seeds) functionality. Performance of two configurations of the PRBs can be defined as the required time for maintaining the concentration of contaminant downgradient of the barrier as less than the maximum copper level (MCL) that could be present in drinking water (0.001 kg/m³) [20]. The C-PRB has a higher operation time (170 d) in comparison with FG-PRB (100 d)
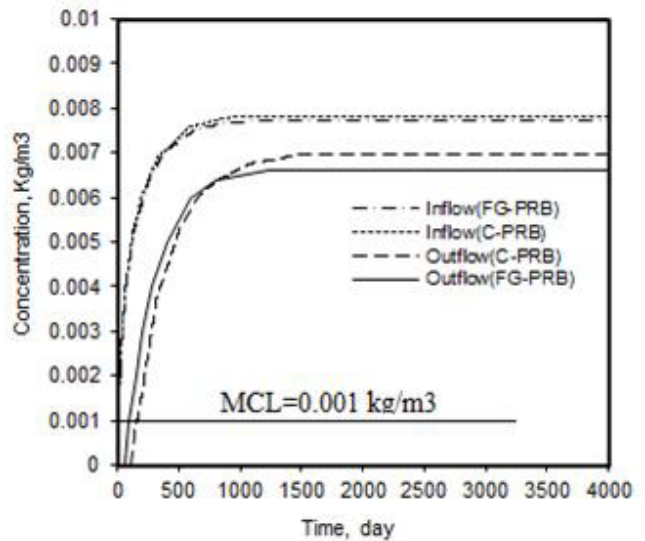

Fig. 9. Copper concentration and time relationship before (inflow) and after (outflow) treatment for C-PRB and FG-PRB.
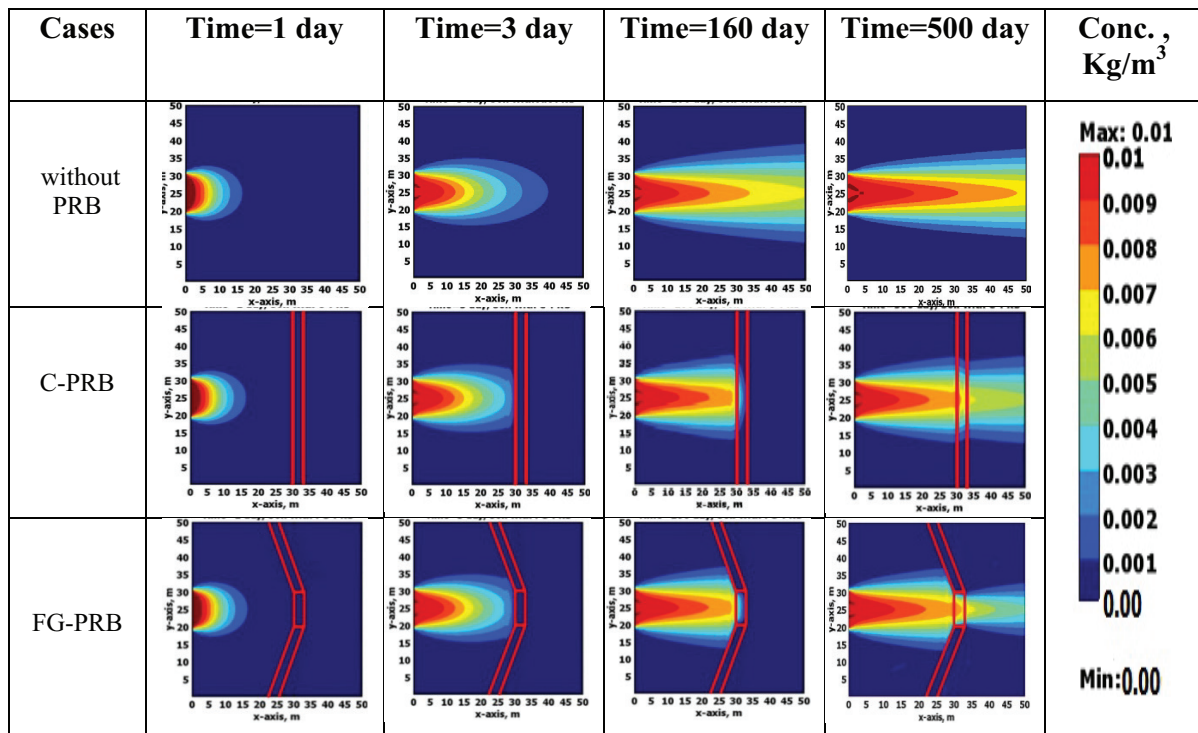

Fig. 8. Contour plot of copper concentration across the model aquifer after various times.
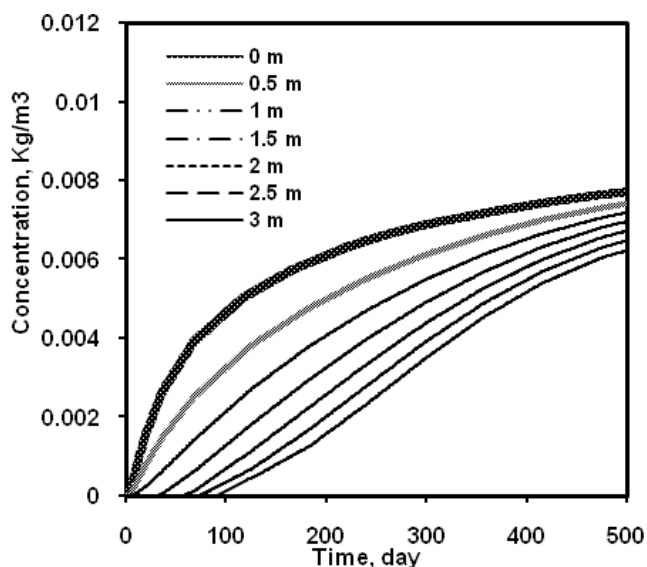
Fig. 10. Copper concentration and time relationship within the thickness of C-PRB.

Fig. 11. The concentration profile of copper being treated with thickness of C-PRB.

since the outflow copper concentration of FG-PRB reached the maximum copper level (MCL) faster than C-PRB as illustrated in Fig. 9. The lower operation time of the FG-PRB is reasonable since the amount of reactive media (olive seeds) used were less than that of the C-PRB.

3.8. Copper removal within C-PRB

Breakthrough curves of copper-contaminated groundwater with the C-PRB are shown in Fig. 10. It is obviously seen that the copper concentration at the front parts of the barrier (e.g., 0.5 m) increases more rapidly than the inner parts (e.g., 2.5 or 3 m). Increase in copper concentration at the front parts of the barrier indicates that the olive seeds have lost its sorption ability. The copper treating performance of any parts of the C-PRB within its thickness of 3 m at different period's time can be depicted in Fig. 11. As mentioned previously that the concentration of copper entering the C-PRB was about 0.0078 kg/m^3. At the front parts of the PRB, it would be in contact first with a high concentration of oncoming groundwater. As a result, the olive seeds at these parts would have reached it sorption ability early and the copper concentration starts increasing. For example, as shown in Fig. 11, the copper concentration at the distance of 0.5 m from the front of the PRB, at 10 d is about 3.38 × 10^{-4} kg/m^3. Later on, at 25 d, the copper concentration becomes 0.001 kg/m^3, and at about 200 d, the concentration becomes approximately 0.005 kg/m^3 and keeps increasing overtime. On the other hand, the olive seeds at the back of the PRB would have reached its sorption ability long after the front ones since it would only be in contact with oncoming groundwater with a lower concentration (e.g., less than 0.0078 kg/m^3) in most of the times of simulation. However, if the constant concentration of source is used, eventually, all parts of the PRB would have reached it sorption ability, and the concentration of the outflow would be equal to the inflow. Finally, for two types of PRBs, the thickness of 3 m
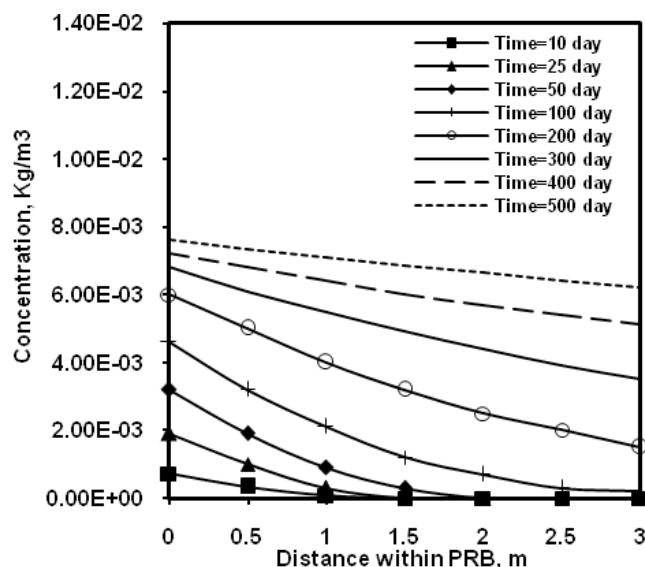
is adequate to treat copper-contaminated groundwater having a concentration not greater than 0.01 kg/m^3 according to the conditions of this study.

4. Conclusions

From the batch experiments, the best values of the parameters that affected copper sorption process onto olive seeds were noted to be contact time of 70 min, initial pH of the solution of 5.5, an initial copper concentration of 10 mg/l, sorbent dosage of 0.8 g/50 ml, and agitation speed of 250 rpm. The sorption data were reasonably well correlated by the Langmuir sorption isotherm with a coefficient of determination (R^2) equal to 0.9971. Furthermore, FTIR analysis proved that the alcohols, carboxylic acids, amines, esters, aromatic, and alkyl halides groups were responsible for removing of copper from the contaminated solution in addition to adsorption process. Distilled water leaching of Copper-bearing olive seeds test indicated that the dissolution of copper is very low. The results of batch experiments, distilled water leaching test, and two-dimensional numerical model confirmed that the olive seeds barrier was efficient in the restriction of contaminant plume and both configurations of PRBs can be used successfully to treat copper-contaminated groundwater with operation time equal to 170 and 100 d for C-PRB and FG-PRB, respectively.

References

[1] P. Kjeldsen, T. Locht, A.P. Karvonen, Removal of TCE and chromate in a permeable reactive barrier using zero-valent iron, International Containment and Remediation Technology Conference and Exhibition 121 (2001) 10–13.
[2] S.W. Wan Ngah, M.A. Hanafiah, Removal of heavy metal ions from wastewater by chemically modified plant wastes as adsorbents: a review, Bioresour. Technol., 99 (2008) 3935–3948.

[3] A. Gavaskar, N. Gupta, B. Sass, R. Janosy, J. Hicks, Final Design Guidance for Application of Permeable Reactive Barriers for Groundwater Remediation, Columbus Ohio Battelle, 2000.

[4] K.E. Roehl, T. Meggyes, F.G. Simon K., D.I. Stewart, Long-term Performance of Permeable Reactive Barriers, New York, Elsevier, 2005.

[5] S. Babel, T.A. Kurniawan, Low-cost adsorbents for heavy metals uptake from contaminated water: a review, J. Hazard. Mater., B97 (2003) 219–243.

[6] Ayad A. H. Faisal, Ziad T. Abd Ali, Remediation of groundwater contaminated with the lead–phenol binary system by granular dead anaerobic sludge-permeable reactive barrier, Environ. Technol., 38(20) (2017) 2534–2542.

[7] A.A. H. Faisal, Z.T. Abd Ali, Using sewage sludge as a permeable reactive barrier for remediation of groundwater contaminated with lead and phenol, Separ. Sci. Technol., 52(4) (2017) 732–742.

[8] A.A.H. Faisal, Effect of pH on the performance of olive pips reactive barrier through the migration of copper-contaminated groundwater, Desal. Water Treat., 57 (2016) 4935–4943.

[9] Z.T. Abd Ali, Using activated carbon developed from Iraqi date palm seeds as permeable reactive barrier for remediation of groundwater contaminated with copper, Al-Khwarizmi Eng. J., 12(2) (2016) 34–44.

[10] S. Yin, G. Herath, S. Heng, S. Kalpage, Using permeable reactive barriers to remediate heavy metal-contaminated groundwater through a laboratory column experiment, Amer. J. Environ. Sci., 13(2) (2017) 103–115.

[11] S.M. Yakout, G. Sharaf El-Deen, Characterization of activated carbon prepared by phosphoric acid activation of olive stones, Arab. J. Chem., 9 (2016) S1155–S1162.

[12] J.P. Chen, L. Wang, S.W. Zou, Determination of lead bio-sorption properties by experimental and modeling simulation study, Chem. Eng. J., 131 (2008) 209–215.

[13] German Standard Methods for the Examination of Water, Waste Water and Sludge and Sediments (Group S), Determination of Leachibility by Water (S4), DIN 38414, Part 4.

[14] S. Wang, Z. Nan, Y. Li, Z. Zhao, The chemical bonding of copper ions on kaolin from Suzhou, China, Desalination, 249 (2009) 991–995.

[15] O.I. Hamdaou, E. Naffrechoux, Modeling of adsorption isotherms of phenol and chlorophenols onto granular activated carbon, J. Hazard. Mater., 147 (2007) 381–394.

[16] C.W. Fetter, Contaminant Hydrogeology. 2nd ed. Prentice-Hall, New Jersey, 1999.

[17] E. Holzbecher, Environmental Modeling Using MATLAB. Springer, Berlin-Heidelberg, 2007.

[18] G.O. El-Sayed, H.A. Dessouki, S.S. Ibrahim, Bio-sorption of Ni(II) and Cd(II) ions from aqueous solutions onto rice straw, Chem. Sci. J., 9 (2010) 1–11.

[19] R. Qadeer, A.H. Rehan, A study of the adsorption of phenol by activated carbon from aqueous solutions, Turk J. Chem., 26 (2002) 357–361.

[20] World Health Organization, Geneva, Guidelines for Drinking Water Quality, Health Criteria, and Other Supporting Information, 2nd ed. vol. 2, 1996.